Exceptional Stability of Azacalixphyrin and Its Dianion

ARTICLE *in* THE JOURNAL OF PHYSICAL CHEMISTRY A · AUGUST 2014

Impact Factor: 2.69 · DOI: 10.1021/jp507485e · Source: PubMed

THE JOURNAL OF PHYSICAL CHEMISTRY A

Article

pubs.acs.org/JPCA

Exceptional Stability of Azacalixphyrin and Its Dianion

Gabriel Marchand,*[,†] Adèle D. Laurent,[†] Zhongrui Chen,[‡] Olivier Siri,[‡] and Denis Jacquemin*[,†,§]

[†]Chimie et Interdisciplinarité: Synthèse, Analyse, Modélisation (CEISAM), UMR CNRS 6230, Université de Nantes, 2 rue de la Houssinière BP 92208, F-44322 Nantes Cedex 3, France

[‡]Centre Interdisciplinaire de Nanoscience de Marseille (CINaM), UMR CNRS 7325, Aix-Marseille Université, Campus de Luminy, case 913, F-13288 Marseille Cedex 09, France

[§]Institut Universitaire de France, 103 bd Saint-Michel, F-75005 Paris Cedex 05, France

Supporting Information

ABSTRACT: Azacalixphyrin is a recently synthesized precursor of potentially highly versatile analogues of porphyrins. Surprisingly, this macrocyclic compound is stable to such an extent that it could be exposed to air for months as a solid or for days in solution without detectable changes. However, no rationalization of this specific property has been established yet as the structure/electronic features of this novel compound are still very much unknown. Here, we present an extensive theoretical study on the stability of azacalixphyrin. We use density functional theory to quantify both its aromaticity and its reactivity, or more precisely its lack thereof, with water. In addition, since we find that neutral azacalixphyrin has the ability to capture easily two electrons, we also discuss the results obtained for its dianion. We show that the azacalixphyrin core is strongly aromatic despite the antiaromatic peripheric rings, and we find that all reactions with water are extremely endergonic, hence explaining the stability of azacalixphyrin. Upon reduction, the aromatic signature is reversed as the center becomes antiaromatic while the antiaromatic character of the peripheric rings is either remarkably reduced or completely annihilated. Accordingly, we find that the reactivity of the dianion with water is considerably inhibited.

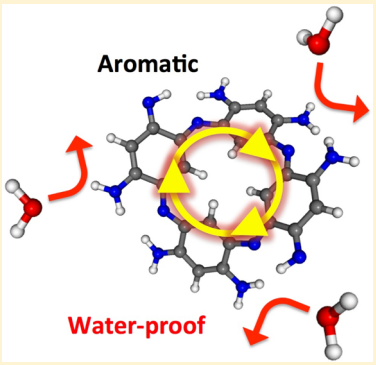

INTRODUCTION

Porphyrins **1** (Scheme 1) belong to a family of macrocyclic molecules with a long and impressive history with application areas ranging from chemistry to material science, physics to biology, and engineering to medicine.[1−10] They are composed of a 16-membered ring with four nitrogen atoms and 18 delocalized π-electrons, implying aromaticity according to the Hückel's rule ($4n + 2 = 18$, with $n = 4$ for the shortest cyclic path). Because of their exceptional versatility, not only in terms of electronic and structural features, but also in terms of synthetic accessibility, porphyrins have been considered a reference molecular basis for the design of a large panel of new families of macrocycles with specific properties.[1−7] Isomers of porphyrins and azaporphyrin derivatives such as porphyrazines and phthalocyanines have indeed been extensively studied.[8−10] For instance, introduction of *meta*-phenylene subunits in hemiporphyrazines have found great interest, especially when the phenyl subunit can be converted to access aromatic conjugation.[11−18]

Scheme 1. Porphyrin 1 and Azacalixphyrin 2

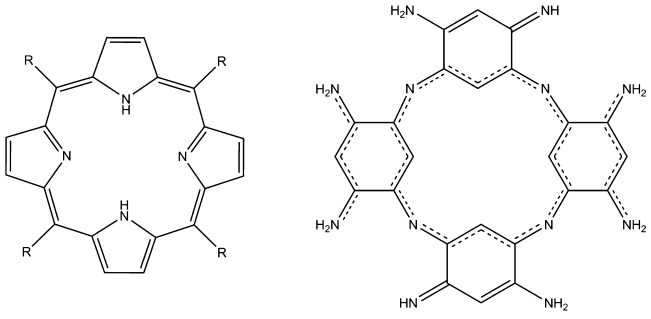

1 **2**

Azacalixphyrin **2** (Scheme 1) is the first member of a new class of isostructural and isoelectronic "pyrrole-free" analogues of porphyrins that can be synthesized in two straightforward steps only.[19] Like **1**, this macrocycle contains four peripheric rings, four nitrogen atoms separated by three carbons, and a 16-membered ring with 18 delocalized π-electrons. It is therefore aromatic and hence stable. An important singularity of **2** compared to other porphyrin analogues is that it is not composed of pyrrole but phenyl subunits. The highly versatile synthetic accessibility of **2** will facilitate the introduction of various substituents on the peripheral nitrogen atoms, which is of utmost importance for the tuning of electronic/structure properties. In addition, as they are NIR-absorbing organic materials (around 900 nm,[19] whereas all free-base porphyrins absorb in the visible range, up to about 700 nm[20]), the potential applications of these macrocycles are diverse and extensive in

Received: July 25, 2014
Revised: August 29, 2014
Published: August 29, 2014

Scheme 2. Hydrolysis Process of 2 in Water; We Focus on the Two Reaction Mechanisms Leading to 3 and 4

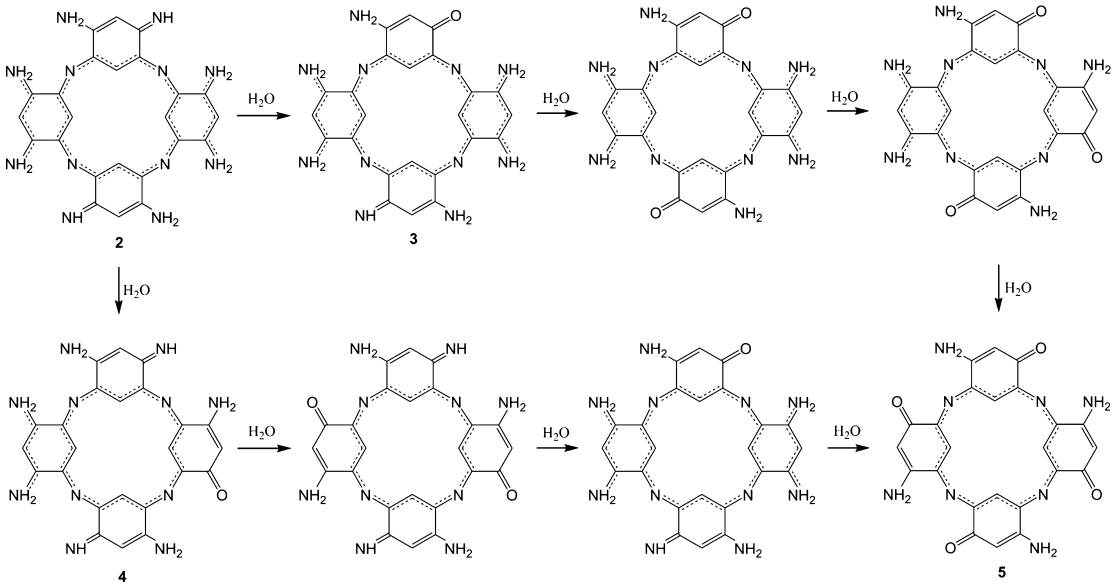

many technological sectors.[21,22] An outstanding versatility by analogy to porphyrins can thus be envisioned for this new class of molecules.

Surprisingly, **2** is stable to such an extent that it could be exposed to air for months as a solid or for days in solution without detectable changes.[19] This exceptional stability is preserved even in the presence of water under air. However, no rationalization of this specific feature has been established yet since the structure/electronic properties of this novel compound are still very much unknown. Here, we present an extensive study on the stability of **2**. More precisely, we use density functional theory (DFT) calculations to quantify both its aromaticity and its reactivity, or actually its lack thereof, with water. A presumed decomposition of **2** in water is the hydrolysis process in Scheme 2; therefore, we investigate the reaction pathways corresponding to the first stage on the two different rings (compounds **3** and **4** in Scheme 2), which are initiated by a protonation step. We further examine the direct decompositions of **2** by protonations and deprotonations on the different NH and NH_2 sites in neutral (H_2O), acid (H_3O^+), and basic (OH^-) media. In addition, since we find that **2** has the ability to capture easily two electrons, we also discuss the results obtained for the dianion $\mathbf{2}^{2-}$.

COMPUTATIONAL METHODS

All calculations have been performed at the DFT level, using the parameter-free PBE0 functional.[23] We used the Gaussian09 package[24] applying default procedures, integration grids, and algorithms, except for tightened SCF (10^{-10} a.u.) and internal forces (10^{-5} a.u.) convergence thresholds. The structures of **2** and $\mathbf{2}^{2-}$ were optimized in their electronic ground states, using the 6-31G(d) atomic basis set. Both the singlet and triplet states were considered, integrating bulk solvent (water) effects with a polarizable continuum model (PCM). Vibrational frequency calculations following geometry optimizations confirmed that the structures are true local minima on the potential energy surface (no imaginary frequencies), except for the transition states between stable geometries (saddle points on the potential energy surface), for which an imaginary frequency was indeed obtained.

On the basis of the optimized structures, single-point calculations were carried out using the 6-31++G(d,p) atomic basis set to correct the total energies. Partial atomic charges were derived using the Merz−Singh−Kollman electrostatic potential fitting procedure.[25] To quantify the aromaticity, we calculated the NICS(0) (nucleus independent chemical shift) at the centroids of all rings, following the methodology proposed by von Schleyer and co-workers.[26] Atomic charges and NICS(0) have been determined with the cc-pVTZ atomic basis set.

Finally, because we found no stationary point for the protonated and deprotonated forms of both **2** and $\mathbf{2}^{2-}$ with, respectively, a hydroxyl and a hydronium around, and similarly, no minimum for the neutral forms together with a H_3O^+ and a OH^-, only barrierless reactions when starting from guess structures could be reached, and we applied a Born−Haber thermodynamic cycle[27,28] to extract the energies of protonations and deprotonations of the different NH and NH_2 sites. Reactants and products were thus optimized separately in the gas phase and additional single-point calculations were carried out using the solvation model density (SMD) of Truhlar and co-workers[29] to estimate solvation energies.

RESULTS AND DISCUSSION

The bridging nitrogens at the periphery of **2** (see Scheme 1) allow the external protons to jump from one nitrogen to another via a hopping mechanism.[19] In total, eight tautomers, differing in their relative positions of the protons at the periphery, are possible. A previous theoretical and experimental work[19] indicates an average (symmetrical) structure that can be explained by a fast interconversion between the tautomers. Here, we focus on the tautomer with the highest degree of symmetry (C_2), namely, the one with the two imines separated by the largest possible distance, therefore minimizing the electrostatic repulsions. Its structure corresponds to that shown in Scheme 1.

Electron Affinities and Ionization Potentials. We first examine the reactivity of neutral azacalixphyrin **2** with an external electrostatic potential, i.e., we calculate the energies of the capture (electron affinities) and the ejection (ionization

dx.doi.org/10.1021/jp507485e | J. Phys. Chem. A 2014, 118, 8883−8888

potentials) of electrons. The resulting energies for the first and second electron affinities and ionization potentials are reported in Table 1. We underline that the vertical and adiabatic energies

Table 1. PCM(water)-PBE0/6-31++G(d,p) First and Second Electron Affinities (EA) and Ionization Potentials (IP) of Azacalixphyrin, in eV; Vertical (vert) and Adiabatic (adia) Values Are Shown

1st EA		2nd EA		1st IP		2nd IP	
vert	adia	vert	adia	vert	adia	vert	adia
−3.59	−3.76	−3.19	−3.37	4.81	4.70	5.25	4.92

are very close (less than 0.2 eV), which suggests that the nuclear geometry of the molecule is mostly unchanged upon oxidation/reduction, most probably because of the high degree of rigidity imposed by the heterocyclic π-conjugation. Both the first and second electronic captures are highly exergonic since the energies associated are strongly negative: −3.76 eV for **2** → $\mathbf{2}^-$ and −3.37 eV for $\mathbf{2}^-$ → $\mathbf{2}^{2-}$. A similar tendency is observed with additional single-point calculations at the second-order Møller−Plesset (MP2) level of theory (see Supporting Information, SI). With respect to the outstanding stability of **2** and although $\mathbf{2}^{2-}$ may not be readily isolated in practice, this promotes $\mathbf{2}^{2-}$ as an even more stable candidate to be taken into account, in contrast to the experimentally unstable dideprotonated form of **2**.[19] Such a flexibility in the degree of reduction is also particularly interesting in the view of designing a macrocycle ligand in the field of coordination chemistry. Extracting one and two electrons from **2** is on the contrary very difficult as it requires a supply of at least 4.70 and 4.92 eV, respectively (see the ionization potentials in Table 1).

The dianion $\mathbf{2}^{2-}$ is expected to be aromatic in its lowest triplet state and antiaromatic in its lowest singlet state since Hückel's rule for aromaticity and antiaromaticity is reversed for triplet states[30] (the first excited triplet state will be aromatic if it has $4n$ π-electrons and antiaromatic if it has $4n + 2$ π-electrons). We thus examine the nature of the electronic ground state of **2** and $\mathbf{2}^{2-}$. After optimizing the structures in both states, we find out that, for both compounds, the energies of the singlets are significantly lower than those of the triplets: 0.44 eV lower for **2** and 0.81 eV lower for $\mathbf{2}^{2-}$. Consequently, **2** must be aromatic, while $\mathbf{2}^{2-}$ must be antiaromatic in its ground state. This will be quantified below, and only singlet states are considered in the following.

Charge Distributions and Structures. The computed charge distributions of **2** and $\mathbf{2}^{2-}$ are shown in Figure 1. Upon reduction from **2** to $\mathbf{2}^{2-}$, most of the excess of negative charge resides at the center of the molecule (a gain of about one electron) and on the merocyanines (side-chains with two NH_2-groups, a gain of 1/2 electron for each). The charge distributions on the cyanines become very close to that of the groups carrying the imines, the latter remaining practically unchanged (0.1 electron only). This behavior predicts a rearrangement of the aromatic pattern and also suggests that the deprotonation of the NH_2 functions will be considerably inhibited for the dianion, while the protonation of the imines will be only slightly favored.

The geometry of **2** has been described experimentally and theoretically in ref 19, and we compare it here with its dianionic analogue. As illustrated in Figure 2, both compounds exhibit a nonplanar saddle conformation because of the repulsion between the central hydrogen atoms. Figure 2 also shows

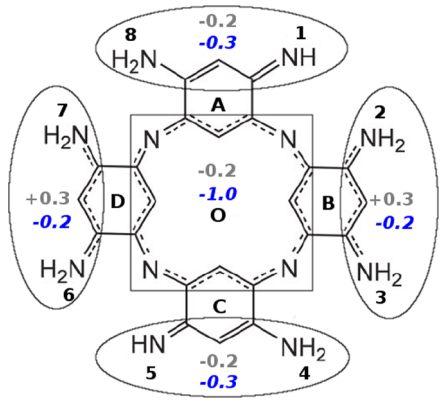

Figure 1. Sums of partial atomic charges (in electrons), derived according to the Merz−Singh−Kollman scheme,[25] within the delimited regions, for **2** (in gray normal font) and $\mathbf{2}^{2-}$ (in blue italic font); at the PCM(water)-PBE0/cc-pVTZ level.

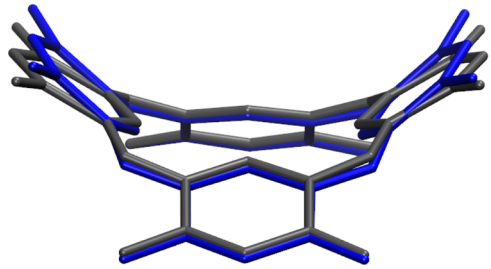

Figure 2. Superimposed geometries of **2** (gray) and $\mathbf{2}^{2-}$ (blue), optimized in their electronic ground state at the PCM(water)-PBE0/6-31G(d) level of theory. Hydrogens are not shown.

that the two structures are very similar as they superimpose almost perfectly, in agreement with the very close vertical and adiabatic electron affinities (see above). However, a significant difference can be seen in the orientation of the rings bearing the cyanine subunits, the dianion adopting a more prominent inclination. This significant conformational change is driven by electrostatic relaxation, as seen from the heterogeneous distribution of the extra negative charge in favor of the cyanines. Compounds **2** and $\mathbf{2}^{2-}$ also differ in their bond length distributions (see the SI), especially, the C−N bonds of the 16-membered ring are homogeneous and about 1.33 Å long for **2**, whereas they alternate between 1.39 and 1.32 Å for $\mathbf{2}^{2-}$. In addition, the bond lengths in the rings containing the cyanines (B and D, see Figure 1) are more homogeneous for the dianion. Together with the charge distributions, this predicts a lower aromaticity for the 16-membered ring and a higher aromaticity for rings B and D upon reduction.

Aromaticity. One likely explanation for the stability of azacalixphyrin is its aromaticity. To quantify the aromaticity of **2** and $\mathbf{2}^{2-}$, we calculated the NICS(0)[26] at the centers of all rings. The NICS values are listed in Table 2, and the naming convention for the rings is shown in Figure 1. The neutral form

Table 2. NICS(0) (in ppm) at the Centers of the Rings of 2 and $\mathbf{2}^{2-}$, Computed at the PCM(water)-PBE0/cc-pVTZ Level; the Indexation of the Rings Is Shown in Figure 1

	O	A	B	C	D
2	−8.0	7.0	3.6	7.0	3.6
$\mathbf{2}^{2-}$	2.2	4.4	−6.4	4.4	−6.4

dx.doi.org/10.1021/jp507485e | J. Phys. Chem. A 2014, 118, 8883−8888

exhibits a strong aromatic character since NICS = −8 ppm at the center of the molecule (ring O). This value is very close to the one reported for highly aromatic compounds, e.g., benzene,[26] and is about half the one of porphyrin.[31] In contrast to porphyrins, where all rings are aromatic, the peripheric rings (A, B, C, and D) of **2** bring instability given their antiaromatic nature. Also, the antiaromaticity of the rings carrying the imine functions (A and C) is considerably more pronounced than that of the rings bearing the cyanines (B and D). This most probably originates in the local inhomogeneity in the electronic distribution induced by the coexistence of the NH and NH_2 groups in A and C, as seen in the bond lengths (see the SI).

The behavior of $\mathbf{2}^{2-}$ is very different from that of **2**. First, it becomes antiaromatic (NICS at the center of the molecule goes from −8.0 to 2.2 ppm), as it was expected for a dianionic singlet ground state.[30] Second, the antiaromatic character of the peripheric rings is either remarkably reduced (from 7.0 to 4.4 ppm for A and C) or completely annihilated (from 3.6 to −6.4 ppm for B and D). These observations are in keeping with the charge and bond length distributions (see above). Such a rearrangement is very interesting in view of stability since azacalixphyrin is presumably more vulnerable to surrounding reactants at its periphery than at its center given: (i) the large radius of such a macrocycle, (ii) the presence of nitrogen atoms at the periphery, and (iii) the phenylic nature of the internal protons that are very poorly acidic.

Reactivity with Water. Azacalixphyrin is very stable in aqueous solution and we therefore examine this exceptional feature. We first investigate the structures and energies involved in the mechanisms of hydrolysis (reaction paths from compound **2** toward compounds **3** and **4**, see Scheme 2). In a second stage, we calculate the thermal free energies ΔG of the protonations and deprotonations on the different NH and NH_2 sites of both **2** and $\mathbf{2}^{2-}$ with neutral (H_2O), acidic (H_3O^+), and basic (OH^-) water following the Born−Haber thermodynamical cycle described in the computational methods section.

Hydrolysis. The structures and energies for the decompositions from **2** to **3** and from **2** to **4** in the presence of a water molecule are shown in Figures 3 and 4, respectively. We find that **3** (+ NH_3) is −2 kcal·mol^{-1} lower in energy than **2** (+ H_2O), and the reaction is therefore thermodynamically favorable. However, the reaction pathway to **3** is very unlikely as it must undergo two successive protonations on the NH function with energy barriers of 42 and 40 kcal·mol^{-1} (see the two transition states in Figure 3), that are very high and therefore prevent degradation. In the presence of a hydronium cation, the first protonation becomes barrierless (geometry optimizations starting from different guess structures of **2** with a H_3O^+ molecule around the NH group systematically lead to the protonated form and H_2O), preserved in acidic water. Beyond that step, the decomposition path to **3** in acid medium (in the SI) is yet clearly prohibited by the presence of an intermediate at 21 kcal·mol^{-1} after the second hydrogen transfer, with a barrier of 49 kcal·mol^{-1}.

The decomposition of **2** via the path leading to **4** in neutral water (Figure 4) is, compared to that giving **3**, even more restricted as the first deprotonation goes through a barrier at 53 kcal·mol^{-1} (against 42 kcal·mol^{-1} through the **3** route). The stationary intermediate is also significantly higher in energy (21 kcal·mol^{-1}, and 10 kcal·mol^{-1} for its equivalent in the reaction giving **3**). This is, however, not surprising given that the protonation takes place on the NH_2 group in the mechanism leading to **4**, while it occurs on the NH group in the mechanism

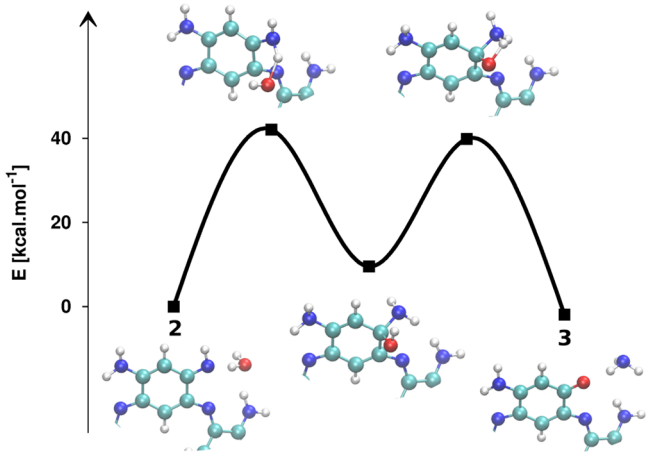

Figure 3. Energies and structures involved in the hydrolysis process leading to compound **3**, from **2** (the reference energy). Maxima on the energy curve correspond to transition states (imaginary frequencies) between two stable structures (no imaginary frequencies) on the energy surface. The curve has been extrapolated from the points using a smoothing function. Only the part of the molecule where the reaction takes place is shown.

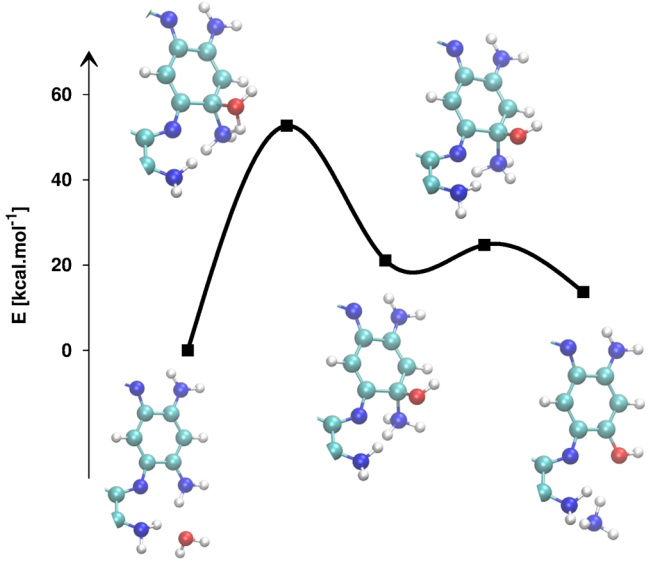

Figure 4. Energies and structures involved in the hydrolysis process leading to the enolic form of compound **4**, from **2** (the reference energy). See caption of Figure 3 for more details.

yielding **3**. For the same reason, the reaction leading to **4** in acidic water will be also inhibited. Finally, no stationary point of the structure of **4** + OH^- could be reached, and the process therefore ends with **4** in its enolic form (+ H_2O), see Figure 4. Extracting the thermal free energy ΔG from the separately optimized reactants (enolic form of **4** and H_2O) and products (**4** and OH^-), we found a very high barrier of 121 kcal·mol^{-1}.

Consequently, the two examined decompositions of azacalixphyrin **2** via hydrolysis in neutral water are not favorable, and similar results can be deduced for the dianion $\mathbf{2}^{2-}$ looking at the protonation energies (see below).

Protonations/Deprotonations. As the first step of the degradation of azacalixphyrin in aqueous solution is the protonation of the NH functions and/or the deprotonation of the NH_2 functions, we compare these reactions at the

dx.doi.org/10.1021/jp507485e | J. Phys. Chem. A 2014, 118, 8883−8888

different sites of azacalixphyrin **2** and its dianion $\mathbf{2}^{2-}$ in the presence of a water molecule (H_2O), and also in acid (for protonations) and basic (for deprotonations) media using hydronium H_3O^+ and hydroxyl OH^- ions, respectively. With H_2O, we found no minima on the electronic ground state potential energy surface for the different protonated (together with OH^-) and deprotonated (together with H_3O^+) forms of both **2** and $\mathbf{2}^{2-}$. The ΔG energies obtained from the separately optimized reactants and products (see Table 3) range from +32 to +79 kcal·mol^{-1}, which are very large endergonic values. In other words, both azacalixphyrin and its dianion are very unlikely to react with water. This stability is, however, not preserved both in acid (as predicted from the hydrolysis mechanisms above) and basic media, the same reactions become largely exergonic (from −6 to −53 kcal·mol^{-1}) and barrierless, due to the strong charge−charge interactions. This is an important information regarding the design of azacalixphyrin through the introduction of adequate substituents capable of tuning its properties. We underline that protonated and deprotonated forms of **2** have been indeed observed from UV/vis/NIR absorption spectra when the molecules were immersed in acid and basic solutions,[19] respectively.

Table 3. Protonation and Deprotonation Energies (in kcal·mol^{-1}) of 2 and $\mathbf{2}^{2-}$ with Water, at T = 298 K (See the Indexation of the Reactive Sites in Figure 1)

	N atom	reaction	ΔG (kcal·mol^{-1})
2	1	$\mathbf{2} + H_2O \rightarrow [\mathbf{2}\cdot H]^+ + OH^-$	38
	1	$\mathbf{2} + H_3O^+ \rightarrow [\mathbf{2}\cdot H]^+ + H_2O$	−43
	5	$[\mathbf{2}\cdot H]^+ + H_2O \rightarrow [\mathbf{2}\cdot 2H]^{2+} + OH^-$	43
	5	$[\mathbf{2}\cdot H]^+ + H_3O^+ \rightarrow [\mathbf{2}\cdot 2H]^{2+} + H_2O$	−38
	2	$\mathbf{2} + H_2O \rightarrow [\mathbf{2} - H]^- + H_3O^+$	49
	2	$\mathbf{2} + OH^- \rightarrow [\mathbf{2} - H]^- + H_2O$	−32
	3	$\mathbf{2} + H_2O \rightarrow [\mathbf{2} - H]^- + H_3O^+$	52
	3	$\mathbf{2} + OH^- \rightarrow [\mathbf{2} - H]^- + H_2O$	−29
	4	$\mathbf{2} + H_2O \rightarrow [\mathbf{2} - H]^- + H_3O^+$	63
	4	$\mathbf{2} + OH^- \rightarrow [\mathbf{2} - H]^- + H_2O$	−18
$\mathbf{2}^{2-}$	1	$\mathbf{2}^{2-} + H_2O \rightarrow [\mathbf{2}\cdot H]^- + OH^-$	32
	1	$\mathbf{2}^{2-} + H_3O^+ \rightarrow [\mathbf{2}\cdot H]^- + H_2O$	−49
	5	$[\mathbf{2}\cdot H]^- + H_2O \rightarrow \mathbf{2}\cdot 2H + OH^-$	34
	5	$[\mathbf{2}\cdot H]^- + H_3O^+ \rightarrow \mathbf{2}\cdot 2H + H_2O$	−47
	2	$\mathbf{2}^{2-} + H_2O \rightarrow [\mathbf{2} - H]^{3-} + H_3O^+$	76
	2	$\mathbf{2}^{2-} + OH^- \rightarrow [\mathbf{2} - H]^{3-} + H_2O$	−5
	3	$\mathbf{2}^{2-} + H_2O \rightarrow [\mathbf{2} - H]^{3-} + H_3O^+$	79
	3	$\mathbf{2}^{2-} + OH^- \rightarrow [\mathbf{2} - H]^{3-} + H_2O$	−2
	4	$\mathbf{2}^{2-} + H_2O \rightarrow [\mathbf{2} - H]^{3-} + H_3O^+$	70
	4	$\mathbf{2}^{2-} + OH^- \rightarrow [\mathbf{2} - H]^{3-} + H_2O$	−11

The least unfavorable reaction in neutral water corresponds to the first imine protonation (accordingly the most favorable case with H_3O^+) with comparable energies for **2** and $\mathbf{2}^{2-}$ (38 and 32 kcal·mol^{-1} with H_2O, −43 and −49 kcal·mol^{-1} with H_3O^+). The reaction energies associated with the deprotonations are much larger, especially for the cyanines of the dianion (compare 49 and 52 to 76 and 79 kcal·mol^{-1} with H_2O, −32 and −29 to −5 and −2 with OH^-). This behavior is in line with the observations based on charge distributions and aromaticity, that is an important capture of the negative charge and a "turned on" aromaticity on the rings carrying the cyanines upon reduction (see above). We can thus conclude that azacalixphyrin is more stable with respect to (de)protonation in aqueous solution in its dianionic form. Furthermore, comparing the energies of deprotonations of **2** with the $NH_2{-}C{=}C{-}C{=}NH_2^+$ cyanine fragment, we can quantify the stabilizing effect owing to the aromatic nature of **2**. The result, the energies for the cyanine reference molecule with H_2O and OH^-, is, respectively, 39 and −42 kcal·mol^{-1}, which is at least 10 kcal·mol^{-1} lower than the corresponding energies of **2**.

CONCLUSIONS

In summary, the stability of the newly designed azacalixphyrin **2**, an isostructural and isoelectronic "pyrrole-free" analogue of porphyrins, has been examined using first-principles calculations. Since the first and second electron affinities of **2** were found to be significantly negative, its dianion $\mathbf{2}^{2-}$ has been considered as well. Both **2** and $\mathbf{2}^{2-}$ exhibit a saddle conformation, with a more pronounced out-of-plane deformation of the rings bearing the NH_2 functions for the dianion. This conformational relaxation is explained by the important contribution of the cyanines in the capture of the two extra electrons. The neutral form of azacalixphyrin is found to be highly aromatic and hence stable. However, all its peripheric rings are antiaromatic. The aromaticity of azacalixphyrin is modified upon reduction as the dianion becomes in overall slightly antiaromatic, while the rings bearing the cyanine subunits become strongly aromatic. The antiaromaticity of the rings carrying the imine functions is also reduced. Such a delocalization of the aromaticity outside the center of the molecule, as explained by the charge and bond length distributions, is particularly interesting in terms of stability since reactions of azacalixphyrin with surrounding molecules are more likely to occur at the periphery. Finally, the reactivity of azacalixphyrin was examined through two hydrolysis mechanisms. Both reaction pathways are found to be very unlikely due to high energy barriers preventing the first protonation steps. In addition, all primary reactions of azacalixphyrin with water (protonations and deprotonations of the different NH_2 and NH groups) presented here are found to be strongly endergonic. This explains why this compound is so stable in neutral aqueous solution. Comparing the energies of deprotonations of **2** with those of the cyanine fragment, we find an energy difference ≥10 kcal·mol^{-1} in favor of the macrocycle, which can be attributed to its aromatic nature. Beyond that, the imine protonations are of comparable energies for both neutral and dianionic forms, while deprotonations of the NH_2 groups require an important amount of extra energy for the dianion, which is hence more stable. This is a direct consequence of the important gain of electrons on the cyanine subunits switching on aromaticity in the corresponding rings upon reduction. Finally, the outstanding stability of both **2** and $\mathbf{2}^{2-}$ is preserved in neutral water only, the protonations and deprotonations in acid (H_3O^+) and basic (OH^-) water presenting no barriers.

dx.doi.org/10.1021/jp507485e | J. Phys. Chem. A 2014, 118, 8883−8888

■ ASSOCIATED CONTENT

Supporting Information

Electron affinities and ionization potentials at the MP2/6-31++G(d,p) level, optimized bond lengths and Cartesian coordinates of **2** and $\mathbf{2}^{2-}$, and hydrolysis process in acidic water. This material is available free of charge via the Internet at http://pubs.acs.org.

■ AUTHOR INFORMATION

Corresponding Authors

*(G.M.) E-mail: gabriel.marchand@univ-nantes.fr.
*(D.J.) E-mail: denis.jacquemin@univ-nantes.fr.

Notes

The authors declare no competing financial interest.

■ ACKNOWLEDGMENTS

G.M. thanks the *Région des Pays de la Loire* for his postdoctoral grant in the framework of the SAPOMAP project. D.J. acknowledges the European Research Council (ERC) and the *Région des Pays de la Loire* for financial support in the framework of a Starting Grant (Marches-278845) and the SAPOMAP project, respectively. This research used resources of the GENCI-CINES/IDRIS (Grant c2013085117), CCIPL (*Centre de Calcul Intensif des Pays de Loire*), and a local Troy cluster. O.S. acknowledges the Centre National de la Recherche Scientifique, the Ministère de la Recherche et des Nouvelles Technologies for financial support and Ph.D. grant of Z.C.

■ REFERENCES

(1) Kadish, K. M.; Smith, K. M.; Guilard, R. *Handbook of Porphyrin Science: With Applications to Chemistry, Physics, Materials Science Engineering, Biology and Medecine*; World Scientific Press: Singapore, 2011.

(2) Vinodh, M.; Alipour, F. H.; Mohamod, A. A.; Al-Azemi, T. F. Molecular Assemblies of Porphyrins and Macrocyclic Receptors: Recent Developments in Their Synthesis and Applications. *Molecules* **2012**, *17*, 11763−11799.

(3) Li, L.-L.; Diau, E. W.-G. Porphyrin-Sensitized Solar Cells. *Chem. Soc. Rev.* **2013**, *42*, 291−304.

(4) Jang, W.-D.; Jeong, Y.-H. Porphyrin-Based Receptors for Selective Ion Bindings. *Supramol. Chem.* **2013**, *25*, 34−40.

(5) Yaku, H.; Murashima, T.; Miyoshi, D.; Sugimoto, N. Specific Binding of Anionic Porphyrin and Phthalocyanine to the G-Quadruplex with a Variety of *in Vitro* and *in Vivo* Applications. *Molecules* **2012**, *17*, 10586−10613.

(6) Bulach, V.; Sguerra, F.; Hosseini, M. W. Porphyrin lanthanide complexes for NIR emission. *Coord. Chem. Rev.* **2012**, *256*, 1468−1478.

(7) Griffith, M. J.; Sunahara, K.; Wagner, P.; Wagner, K.; Wallace, G. G.; Officer, D. L.; Furube, A.; Katoh, R.; Mori, R.; Mozer, A. J. Porphyrins for dye-sensitised solar cells: new insights into efficiency-determining electron transfer steps. *Chem. Commun.* **2012**, *48*, 4145−4162.

(8) Vogel, E.; Köcher, M.; Schmickler, H.; Lex, J. Porphycene-a Novel Porphyrin Isomer. *Angew. Chem., Int. Ed.* **1986**, *25*, 257−259.

(9) Sánchez-García, D.; Sessler, J. L. Porphycenes: synthesis and derivatives. *Chem. Soc. Rev.* **2008**, *37*, 215−232.

(10) Vogel, E.; Jux, N.; Rodriguez-Val, E.; Lex, J.; Schmickler, H. Porphyrin Homologues: [22]Porphyrin(2.2.2.2), a "Stretched Porphycene". *Angew. Chem., Int. Ed. Engl.* **1990**, *29*, 1387−1390.

(11) Jianzhuang, J. *Functional Phthalocyanine Molecular Materials (Structure and Bonding)*; Springer: Berlin, Germany, 2010.

(12) Wu, R.; Çetin, A.; Durfee, W. S.; Ziegler, C. J. Metal-Mediated C−H Bond Activation in a Carbon-Substituted Hemiporphyrazine. *Angew. Chem., Int. Ed.* **2006**, *45*, 5670−5673.

(13) Çetin, A.; Durfee, W. S.; Ziegler, C. J. Low-Coordinate Transition-Metal Complexes of a Carbon-Substituted Hemiporphyrazine. *Inorg. Chem.* **2007**, *46*, 6239−6241.

(14) Sripothongnak, S.; Pischera, A. M.; Espe, M. P.; Durfee, W. S.; Ziegler, C. J. Synthesis and Characterization of Lithium Hemiporphyrazines. *Inorg. Chem.* **2009**, *48*, 1293−1300.

(15) Sripothongnak, S.; Barone, N.; Ziegler, C. J. C−H Bond Activation and Ring Oxidation in Nickel Carbahemiporphyrazines. *Chem. Commun.* **2009**, *30*, 4584−4586.

(16) Çetin, A.; Sripothongnak, S.; Kawa, M.; Durfee, W. S.; Ziegler, C. J. Co(II) and Co(III) Complexes of *m*-Benziphthalocyanine. *Chem. Commun.* **2007**, *41*, 4289−4290.

(17) Muranaka, A.; Ohira, S.; Hashizume, D.; Koshino, H.; Kyotani, F.; Hirayama, M.; Uchiyama, M. [18]/[20]π Hemiporphyrazine: A Redox-Switchable Near-Infrared Dye. *J. Am. Chem. Soc.* **2012**, *134*, 190−193.

(18) Lash, T. D. Oxybenziporphyrin, a Fully Aromatic Semiquinone Porphyrin Analog with Pathways for 18π-Electron Delocalization. *Angew. Chem., Int. Ed.* **1995**, *34*, 2533−2535.

(19) Chen, Z.; Giorgi, M.; Jacquemin, D.; Elhabiri, M.; Siri, O. Azacalixphyrin: The Hidden Porphyrin Cousin Brought to Light. *Angew. Chem., Int. Ed.* **2013**, *52*, 6250−6254.

(20) Gouterman, M. Spectra of Porphyrins. *J. Mol. Spectrosc.* **1961**, *6*, 138−163.

(21) Qian, G.; Wang, Z. Y. Near-Infrared Organic Compounds and Emerging Applications. *Chem.—Asian. J.* **2010**, *5*, 1006−1029.

(22) Jiang, H. Organic Ambipolar Conjugated Molecules for Electronics: Synthesis and Structure−Property Relationships. *Macromol. Rapid Commun.* **2010**, *31*, 2007−2034.

(23) Adamo, C.; Barone, V. Toward Reliable Density Functional Methods without Adjustable Parameters: The PBE0 Model. *J. Chem. Phys.* **1999**, *110*, 6158−6169.

(24) Frisch, M. J.; Trucks, G. W.; Schlegel, H. B.; Scuseria, G. E.; Robb, M. A.; Cheeseman, J. R.; Scalmani, G.; Barone, V.; Mennucci, B.; Petersson, G. A.; et al. *Gaussian 09*, revision A.02; Gaussian, Inc.: Wallingford, CT, 2009.

(25) Singh, U. C.; Kollman, P. A. An Approach to Computing Electrostatic Charges for Molecules. *J. Comput. Chem.* **1984**, *5*, 129−145.

(26) Chen, Z.; Wannere, C. S.; Corminboeuf, C.; Puchta, R.; v. R. Schleyer, P. Nucleus-Independent Chemical Shifts (NICS) as an Aromaticity Criterion. *Chem. Rev.* **2005**, *105*, 3842−3888.

(27) Born, M. A Thermochemical Application of the Lattice Theory. *Ver. Dtsch. Phys. Ges.* **1919**, *21*, 13−24.

(28) Haber, F. Reflections on the Theory of Heat Tint. *Ver. Dtsch. Phys. Ges.* **1919**, *21*, 750−768.

(29) Marenich, A. V.; Cramer, C. J.; Truhlar, D. G. Universal Solvation Model Based on Solute Electron Density and on a Continuum Model of the Solvent Defined by the Bulk Dielectric Constant and Atomic Surface Tensions. *J. Phys. Chem. B* **2009**, *113*, 6378−6396.

(30) Baird, N. C. Quantum Organic Photochemistry. II. Resonance and Aromaticity in the Lowest 3.pi..pi.* State of Cyclic Hydrocarbons. *J. Am. Chem. Soc.* **1972**, *94*, 4941−4948.

(31) Kiran, B.; Nguyen, M. T. Density Functional Studies on N-Fused Porphyrin. Electronic, Magnetic and Metal Binding Properties. *J. Organomet. Chem.* **2002**, *643*−*644*, 265−271.